Apoptosis (2012) 17:749–761
DOI 10.1007/s10495-012-0734-1

ORIGINAL PAPER

TSSC3 overexpression reduces stemness and induces apoptosis of osteosarcoma tumor-initiating cells

Yusheng Huang · Huanzi Dai · Qiao-Nan Guo

Published online: 19 May 2012

Abstract Osteosarcoma (OS) is the most common primary bone tumor in children and adolescents, typically presenting with poor prognosis. Recent studies suggested that tumor initiating cells (T-ICs) drive tumor formation and relapse or metastasis and are relatively resistant to cell death induced by conventional chemo- and radiotherapies. Therefore, the poor prognosis of OS appears to be associated with T-ICs. Here, we enriched T-ICs in OS cell lines and evaluated whether the imprinted gene TSSC3 (tumor-suppressing STF cDNA 3) associated with apoptosis could affect T-ICs in OS. Sarcosphere selection and serial clone-forming unit assays were successfully used to enrich T-ICs from OS cell lines. Enrichment of T-ICs from a malignantly transformed hFOB1.19 osteoblast cell line (MThFOB1.19) indicated that OS T-ICs could originate from differentiated cells, and most of these MThFOB1.19 cells showed stem-like features. TSSC3 was expressed at a low level in T-ICs, while overexpression of TSSC3 could efficiently downregulate the expression of stem cell markers Nanog, Oct4 and Sox2 in T-ICs and decrease the clone formation rate, as well as downregulate tumorigenesis in MThFOB1.19 cells, supporting a suppressive role for TSSC3 in OS T-ICs. Furthermore, overexpression of TSSC3 was found to induce apoptosis of OS T-ICs through increasing cleaved caspase-3 (active form), increasing the release of Cyt *c* and decreasing pro-caspase-9 (pro-enzyme form), as well as disruption of the mitochondrial membrane potential ($\Delta\Psi$). Taken together, our findings provide preliminary evidence that TSSC3 inhibits OS tumorigenicity through reducing stemness and promoting apoptosis of T-ICs. Thus, targeting TSSC3 may be a promising approach to suppressing tumorigenicity in OS.

Keywords Tumor-initiating cell · Apoptosis · TSSC3 · Osteosarcoma

Abbreviations

$\Delta\Psi$	Membrane potential (mitochondrial)
DMEM	Dulbecco's minimal essential medium
FBS	Fetal bovine serum
OS	Osteosarcoma
PI	Propidium iodide
T-ICs	Tumor initiating cells
TSCs	Tumor stem cells
TSSC3	Tumor-suppressing STF cDNA 3

Introduction

Osteosarcoma (OS) is one of the most common primary malignant tumors of the bone. High incidence rates of lung metastasis renders this malignant tumor particularly refractory to standard therapies. Emerging lines of evidence have confirmed that tumor stem cells (TSCs) or tumor initiating cells (T-ICs) drive tumor initiation and tumor relapse or metastasis [1–4]. T-ICs are a small subset of cancer cells, which constitute a reservoir of self-sustaining cells with the exclusive ability to self-renew and maintain the tumor [3, 5]. These T-ICs have been proposed to arise either from normal stem cells and progenitor or terminally differentiated cells [5, 6]. Recent studies

Yusheng Huang and Huanzi Dai contributed equally to this study.

Y. Huang · H. Dai · Q.-N. Guo (✉)
Institute of Pathology and Southwest Cancer Center, Southwest Hospital, Third Military Medical University, 400038 Chongqing, China
e-mail: qiaonan85@263.net

indicate that solid tumors of different origins, including OS, are also driven by TSCs or T-ICs. OS may arise from either mesenchymal stem cells (MSCs) or osteoprogenitors [7]. Although human OS T-ICs have not been fully characterized, such stem-like tumor cells are thought to play a key role in chemoresistance and metastasis of OS [8]. Improved targeted gene therapies and chemosensitization strategies are therefore needed to eradicate T-ICs in OS.

Since Gibbs et al. [9] first identified a subpopulation of stem-like cells in bone sarcomas using a neurosphere culture system, the existence of T-ICs in OS have been confirmed in different cell lines and human specimens by various means [10–13]. Although the methods utilized to detect OS T-ICs show populations with enriched stem cell-like characteristics, no specific markers for OS T-ICs have been established. The expressions of stem cell-like markers, such as Oct4, Nanog and Sox2, are always upregulated in T-ICs [9, 12, 14, 15]; however, it is inconvenient to use these markers for isolation. Furthermore, most commonly used human osteosarcoma cell lines, such as SaOS2, MG63 and U2OS cells, do not grow efficiently in animal models, hindering further research on the in vivo tumorigenic ability of isolated T-ICs and confirm their stem cell nature. Investigation of biological characteristics of T-ICs will require the establishment of appropriate OS models. Recent studies have shown that poorly differentiated human tumors contain higher numbers of T-ICs than well-differentiated tumors [16], which can be verified by testing their in vivo tumorigenicity.

Alterations of chromosomal regions, inactivation of tumor suppressor genes and the deregulation of major signaling pathways have been implicated in OS formation and progression [7]. Our previous study revealed that changes in expression of imprinted oncogenes are involved in OS tumorigenesis [17]. Among them, overexpression of TSSC3 (tumor-suppressing STF cDNA 3), the first apoptosis-related gene found to be imprinted [18], was associated with growth inhibition and apoptotic induction in human OS [19]. Whether TSSC3 plays a role in the generation or affects the behavior of OS T-ICs remains unknown.

In the present study, we successfully used two different methods to enrich T-ICs in OS cell lines, MG63, SaOS2 and a poorly differentiated OS cell line, MThFOB1.19, which was malignantly transformed by our lab from the osteoblast cell line hFOB1.19 [17]. Our results demonstrated that OS T-ICs could originate from differentiated osteoblast cells, and most MThFOB1.19 cells showed stem-like features. Additionally, overexpression of TSSC3 could inhibit OS tumorigenicity through reducing T-IC stemness and inducing apoptosis in this cell population.

Materials and methods

Cell culture

MThFOB1.19 cells were established in our lab, treated sequentially by an initiating factor, *N*-methyl-*N*′-nitro-*N*-nitrosoguanidine (MNNG), and a promoter, 12-O-tetradecanoyl phorbol-13-acetate (TPA), as described previously [17]. Cells were cultured in Dulbecco's minimal essential medium (DMEM)/Ham's F12 medium (Hyclone, Logan, UT, USA), supplemented with 10 % fetal bovine serum (FBS, Gibco, Grand Island, NY, USA), 100 U/ml penicillin G (Gibco) and 100 U/ml streptomycin (Gibco). Human OS cell lines SaOS2 and MG63 were obtained from American Type Culture Collection (ATCC, Manassas, VA, USA) and maintained in RPMI1640 (Gibco) with 10 % FBS (Gibco).

Sarcosphere formation assay

MThFOB1.19, MG63 and SaOS2 cells were seeded in 96-well plates (Corning Costar, Corning, NY, USA) at 1 cell/well with 100 μl stem cell medium consisting of DMEM/F12 (Gibco), B27 (1× Gibco), recombinant human epidermal growth factor (rhEGF, 20 ng/ml, Sigma, St. Louis, MO, USA), basic fibroblast growth factor (bFGF, 20 ng/ml, Sigma, USA). The stem cell medium was changed every 3 days, and cells were observed every day by microscopy. After the primary tumor spheres reached approximately 100–150 cells/sphere, they were dissociated and replanted into 96-well plates with 1 cell/well cultured with stem cell medium. The secondary spheres derived from single cells of the primary tumor spheres were examined by microscopy.

Serial clonogenic assay

To determine ability of the cells to self-renew, single-cell suspensions were prepared as described previously [20]. The cells were seeded in 96-well plates (Corning Costar) at a density of 1 cell/well and cultured in complete growth medium supplemented with 10 % FBS. Clones were observed daily under the microscope, and wells containing no cells or more than 1 cell were excluded. After most cell clones expanded to >200 cells, the cells were dissociated and replanted in new 96-well plates to generate subclones.

Tumorigenic assay

Cells were injected subcutaneously (s.c., 5×10^5, 5×10^4) into 4-week-old female nude mice (Center of Experimental Animals, Third Military Medical University, Chongqing, China). Mice were treated according to the

guidelines of the Third Military Medical University Animal Committee. Tumor formation was examined every day. The mice were sacrificed 6 weeks after implantation.

Adipogenic differentiation and oil red O staining

Induction of adipogenesis in MThFOB1.19 cells was performed in Human Mesenchymal Stem Cell Adipogenic Differentiation Medium according to the manufacturer's protocol (Cyagen, Shanghai, China). In brief, cells were plated in 6-well plates (Corning Costar) the day before the initiation of adipogenesis by incubation in solution A for 72 h. Solution A was changed to solution B for 24 h and then switched to solution A again. After alternating incubations with these two media solutions three times, cells were incubated in solution A for an additional 72 h. Subsequently, cells were fixed with 4 % paraformaldehyde (PFA) and then stained with filtered Oil Red O solution (0.3 % Oil Red O in 60 % isopropanol) for 15 min. The nuclei were stained with hematoxylin.

Real-time PCR analysis

Total RNA was extracted from cells using Trizol reagent (TaKaRa, Dalian, China) according to the manufacturer's protocol. Total RNA was reverse transcribed by using the PrimeScript RT Reagent Kit (TaKaRa). Real-time PCR was performed with SYBR PrimeScript RT-PCR Kit (TaKaRa) according to the manufacturer's instructions. Real-time PCR cycles were as follows: initiation with a 3-min denaturation at 95 °C, followed by 40 amplification cycles with 15 s of denaturation at 95 °C, 30 s of annealing at 60 °C and 30 s of extension at 72 °C, levels of expression were normalized to the glyceraldehyde-3-phosphate dehydrogenase (GAPDH) housekeeping gene. The examined genes and their PCR primers are listed in Table 1.

Table 1 Primer sequences for real-time PCR

Gene	Primer sequences	Product size
GAPDH	5′CTTTGGTATCGTGGAAGGACTC3′	132
	5′GTAGAGGCAGGGATGATGTTCT3′	
Nanog	5′TTTGTGGGCCTGAAGAAAACT3′	116
	5′AGGGCTGTCCTGAATAAGCAG3′	
Oct4	5′GCAGCGACTATGCACAACGA3′	195
	5′CCAGAGTGGTGACGGAGACA3′	
Sox2	5′CATCACCCACAGCAAATGACA3′	242
	5′GCTCCTACCGTACCACTAGAACTT3′	
TSSC3	5′TCCAGCTATGGAAGAAGAAGC3′	163
	5′GTGGTGACGATGGTGAAGTACA3′	
Bak	5′CCCACTCAACAGCAAAGA3′	126
	5′ATGGAGAAGGGCAGCAAG3′	
Bim	5′CAGACAGAGCCACAAGGT3′	138
	5′AAAGATGAAAAGCGGGGA3′	
Bax	5′CATCGGGGACGAACTGGA3′	310
	5′GTGGGGGTGAGGAGGCTT3′	
Bcl2	5′GCGGAGTTCACAGCTCTATAC3′	136
	5′AAAAGGCCCCTACAGTTACCA3′	
Cytc	5′TCGGAGCGGGAGTGTTCGTTG3′	122
	5′CCTCCCTTTTCAACGGTGTGGC3′	
Apaf-1	5′ATGGCAGGCTGTGGGAAG3′	230
	5′ATCAGAATGCGGAGACGG3′	
Noxa	5′CAAGAACGCTCAACCGA3′	142
	5′GGTTCCTGAGCAGAAGAGTT3′	
Puma	5′CTCAGCCCTCGCTCTCGC3′	166
	5′AGGTCGTCCGCCATCCGC3′	
Fas	5′TATCACCACTATTGCTGGAGTCA3′	117
	5′GCTGTGTCTTGGACATTGTCA3′	
FasL	5′GAACTCCGAGAGTCTACCAGC3′	119
	5′TTGCCTGTTAAATGGGCCACT3′	
Flip	5′ACAACAAGGACCACGGGAGGAG3′	99
	5′TGGAGGCAAAGAAACCGAAAGC3′	
Caspase3	5′GCGAATCAATGGACTCTGGAAT3′	151
	5′AGGTTTGCTGCATCGACATCTG3′	

Immunofluorescence

For immunofluorescence staining, cell suspensions were seeded onto glass coverslips in DMEM with 10 % FBS for 24 h. The cells were then fixed with 4 % PFA and blocked with normal goat serum (Zhongshan, Peking, China). The cells were washed three times with 0.01 M PBS and then incubated with antibodies to TSSC3 (goat polyclonal IgG, 1:100 dilution; Santa Cruz Biotechnology, Inc., Santa Cruz, CA, USA), Nanog (mouse monoclonal IgG, 1:500, Abcam, Hong Kong, China), Oct4 (mouse monoclonal IgG, 1:500, Abcam), Sox2 (mouse monoclonal IgG, 1:500, Abcam), Bcl2 (rabbit polyclonal IgG, 1:50 dilution; Santa Cruz), pro-caspase-8 (rabbit polyclonal IgG, 1:50 dilution; Santa Cruz) and pro-caspase-9 (rabbit polyclonal IgG, 1:50 dilution; Santa Cruz) at 4 °C overnight, followed by detection with appropriate secondary antibodies (Cy3 Red goat anti-mouse, Cy3 Red goat anti-rabbit, and FITC Green rabbit anti-goat; Boster, Wuhan, China). The cells were counterstained with Hochest33342 (Beyotime, Shanghai, China) to visualize nuclei. Finally, the coverslips were analyzed by laser confocal scanning microscopy (SP-5, Leica, Mannheim, Germany).

Overexpression of TSSC3

The GeneSwitch™ system (Invitrogen, Carlsbad, CA, USA) was kindly provided by Chen Qian (Institute of Pathology, Southwest Hospital, Third Military Medical

University, Chongqing, China) and was used for overexpression of TSSC3. The sequence information of human TSSC3 was obtained from Genbank (NM_001753), and the CDS of TSSC3 was amplified by primers 5′- CCC AAGCTTATGAAATCCCCCGACGAG -3′ and 5′-CGG GATCCTCATGGCGTGCGGGGTTT-3′ for 35 cycles with 50 °C as the annealing temperature. The Pgene/V5-His vector and PCR products were digested with HindIII and BamHI (Takara) and ligated together by T4 DNA ligase (Takara). Positive recombinant clones were isolated and sequenced with an ABI PRISM 377 DNA Sequencer at Invitrogen Biotech Company (Shanghai, China). The Pgene/V5-His and pSwitch vectors were then co-transfected into MThFOB1.19 cells, which were selected with 100 μg/ml Zeocin (Invitrogen) and 300 μg/ml Hygromycin B (Invitrogen), and induced with 50 nM mifepristone (Invitrogen) to express TSSC3. The MThFOB1.19 cells stably transfected with Pgene/V5-His/TSSC3 and Pgene/V5-His/control were designated as overTSSC3 and overCON cells, respectively.

Apoptosis assay

Annexin V-APC/Propidium Iodide (PI) assay

Apoptotic cells were identified by using the Annexin V-APC/PI kit (Becton–Dickinson, Franklin Lakes, NJ, USA) according to the manufacturer's instructions. Briefly, cells were harvested and resuspended in 200 μl binding buffer containing 5 μl Annexin V-APC (20 μg/ml) and 5 μl PI (50 μg/ml). Cells stained with Annexin V-APC only, cells stained with PI (propidium iodide) only and unstained cells were used as controls. Cells were incubated for 15 min at room temperature in the dark. Flow cytometric analysis was performed using a FACscalibur (Becton–Dickinson, Franklin lakes, NJ, USA). Each experiment was repeated at least three times to ensure reproducibility. Annexin V-APC positive, PI negative cells were identified as early apoptotic cells. Annexin V-APC and PI positive cells were identified as late apoptotic cells or necrotic cells

Mitochondrial membrane potential ($\Delta\Psi$) analysis

Mitochondrial transmembrane potential were examined using a Mitochondrial Membrane Potential Assay Kit (Beyotime Institute of Biotechnology, Haimen, China) with JC-1 (lipophilic cation 5,5′,6,6′-tetrachloro-1,1′,3,3′-tetraethylbenzimidazolcarbocyanine iodide). Briefly, overCON sphere cells and overTSSC3 sphere cells were dissociated, and single cells were seeded into poly-L-lysine (Sigma) coated 6-well plates at 5×10^5 cells/well. After culturing in DMEM with 10 % FBS for 4 h in a CO_2 incubator, the cells were incubated with 1 ml JC-1 working solution in the CO_2 incubator for 20 min. The staining solution was removed, and cells were washed with JC-1 staining buffer twice before being analyzed by fluorescence microscopy using a band-pass filter (Fluorescein and Cy3). The depolarizing agent CCCP (10 μM) was used as a positive control.

Western blot analysis

Total proteins were extracted from cells by treatment with lysis buffer [10 mM Tris–HCl, pH 7.4, 150 mM NaCl, 1 mM EDTA, 1 % Nonidet P-40, 1 % Triton-X, and Halt Protease and Phosphatase Inhibitor Cocktail (Pierce, Rockford, IL, USA)]. Protein concentrations were measured using the BCA Protein Assay Reagent (Pierce, Rockford, IL, USA). Approximately 30 μg of total protein were separated by 10 % SDS–polyacrylamide gels and transferred to PVDF membranes (Invitrogen). After blocking, membranes were incubated with primary antibody against TSSC3 (rabbit polyclonal IgG, 1:100 dilution; Abcam), Cytochrome *C* (Cyt *c*, mouse monoclonal IgG, 1:500 dilution; Abcam), pro-caspase-3 (rabbit monoclonal IgG, 1:100 dilution; Santa Cruz) or *β*-actin (mouse monoclonal IgG, 1:500 dilution; Abcam) overnight. Then the membranes were incubated with secondary antibody (anti-mouse or anti-rabbit IgG at a 1:2,000 dilution; Zhongshan, China), and immune complexes were detected using an ECL Kit (Pierce). Finally, the results were analyzed with Image LabTM Software (Bio-Rad), and all the targeted genes were normalized to *β*-actin.

Statistical analysis

All experiments were repeated at least three times. Mean values and standard deviations were calculated. Statistical analyses were performed using the SPSS13.0 statistical software. $P < 0.05$ was considered statistically significant.

Results

MThFOB1.19 cell line has a higher sarcosphere formation ability compared with SaOS2 and MG63 cell lines

An important feature of T-ICs is the capacity to form spheres in stem cell medium [4]. Therefore, the sarcosphere formation assay was used to culture T-ICs in different OS cell lines. Cultured with stem cell medium in 96-well plates, tumor spheres containing 10–20 cells from 1 cell/well were observed after 5–6 days (Fig. 1a, top).

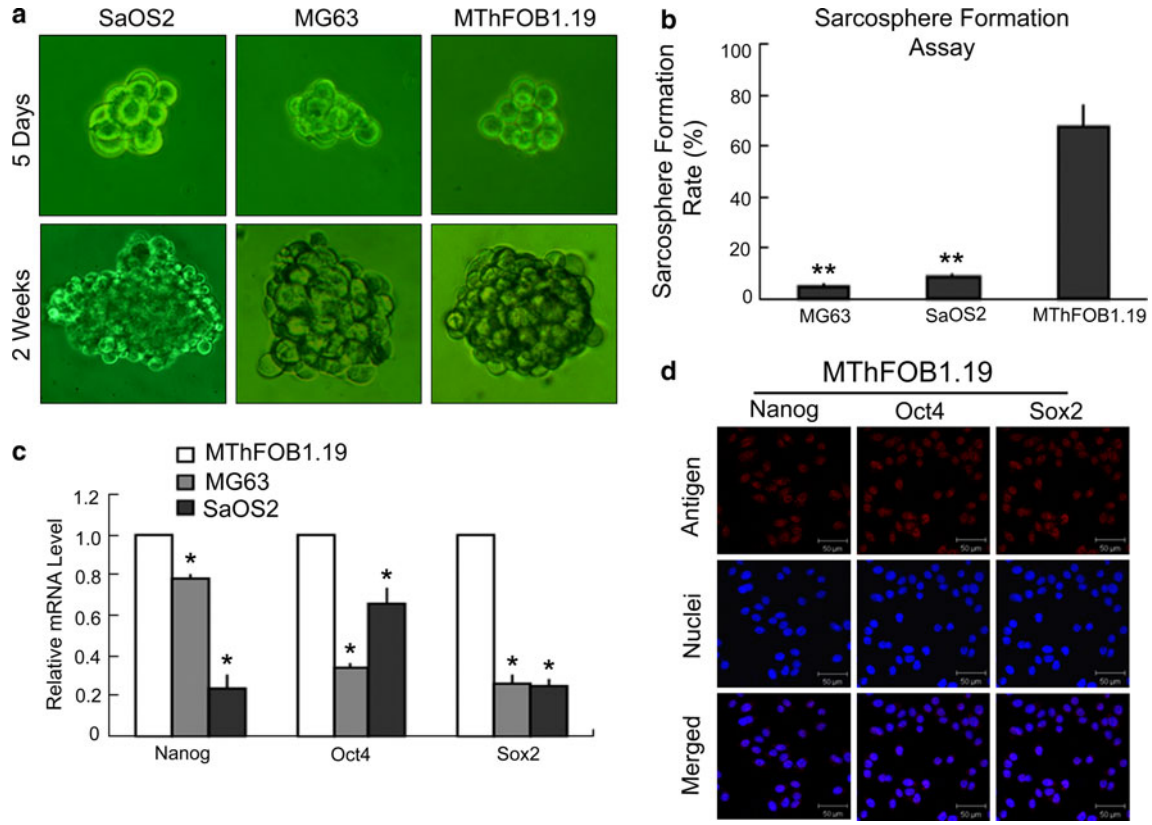

Fig. 1 MThFOB1.19 cell line has a high sarcosphere formation ability. **a** MG63, Saos2 and MThFOB1.19 cells were cultured in stem cell medium in 96-well plates with 1 cell/well. Sarcospheres containing 10–20 cells were observed after 5 days (*top*, magnification, ×200). Within 2 weeks, the diameter of these spheres increased by 10- to 20-fold (*bottom*, magnification, ×200). **b** Sarcosphere formation rate of MThFOB1.19 cells was much higher than that of SaOS2 and MG63 cells. $^{**}P < 0.01$ vs. MThFOB1.19 cells; *bars*, SD. **c** Expressions of stem cell markers in MThFOB1.19 cells were much higher than those of SaOS2 and MG63 cells at the transcriptional level. $^{*}P < 0.05$ vs. MThFOB1.19 cells; *bars*, SD. **d** Expressions of stem cell markers Nanog, Oct4 and Sox2 in MTfFOB1.19 cells detected by immunofluorescence, revealed that these markers were expressed in MThFOb1.19 cells and localized primarily to the nucleus. *Scale bar* = 50 μm

After 2 weeks, the diameter of these spheres increased by 10- to 20-fold (Fig. 1a, bottom). The tumor sphere formation rate of MThFOB1.19 cells was 67.09 ± 9.28 %, obviously higher than that of MG63 (5.40 ± 1.06 %) and SaOS2 (8.60 ± 1.16 %) cells (Fig. 1b; $P < 0.01$).

It has been reported that stem cell markers Nanog, Oct4 and Sox2 play important roles in maintaining the self-renewal and propagation of cells [20]. Therefore, we asked whether OS with different sarcosphere formation abilities had different expression patterns for these factors. By real-time PCR analysis of different OS cell lines, the Nanog, Oct4 and Sox2 transcripts were found to be highly expressed in MThFOB1.19 cells compared with MG63 and SaOS2 cells (Fig. 1c). Immunofluorescence was also used to detect these markers at the protein level in the above cell lines, which showed that they were indeed expressed in MThFOb1.19 cells and localized primarily to the nucleus (Fig. 1d), while there was little to no expression in MG63 and SaOS2 cells (data not shown).

MThFOB1.19 cell line is mainly composed of T-ICs

Zheng et al. [21] reported that clonal and population analyses can be used to investigate the proportion of T-ICs in cancers. We found that MThFOB1.19 cells in normal culture conditions displayed remarkably clone-like growth characteristics at a low cell density (Fig. 2a, left). Therefore, analyses of serial clonal formation and clonal tumorigenicity were used to evaluate the T-ICs in MThFOB1.19 cells. From single MThFOB1.19 cells seeded in 96-well plates by limiting dilution, we obtained 61 clones consisting of 200–400 cells originating from individuals cells after 2 weeks of culture (Fig. 2a, middle). The primary clones were subcultured by dissociating the cells and planting them individually into 96-well plates again. The 110 primary clones generated 102 subclones after 2 weeks of culturing in the same way. The primary clone and subclone formation rates were 100 % and 92.7 ± 4.29 %, respectively. Subsequently, 5×10^5 ($n = 4$) or 5×10^4

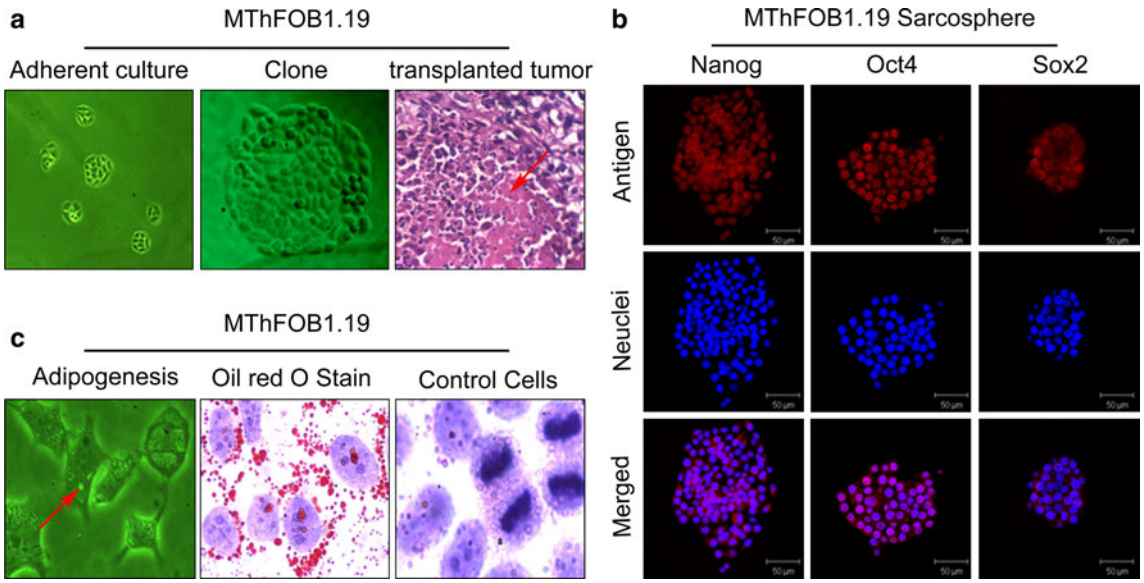

Fig. 2 Pluripotency of MThFOB1.19 cells. **a** MThFOB1.19 cells displayed clone-like growth characteristics when the cell density was low in normal attachment culture (*left*, magnification, ×100). When planted in 96-well plates at a density of 1 cell/well, most cells generated a clone within 2 weeks (*middle*, magnification, ×200). Tumors were observed at 2 weeks after injection of clones or subclones, which had been expanded in six-well plates, into nude mice. Histological analysis showed that these tumors contained numerous hyperchromatic nuclei with pleomorphism. The *arrow* indicates abundant necrosis in the tumor (*right*, magnification, ×200). **b** The expression of Nanog, Oct4 and Sox2 in sarcospheres. *Scale bar* = 50 μm. **c** After adipogenic induction, MThFOB1.19 cells showed enlarged cell volume, increased cytoplasm and lower karyoplasmic ratio. The *arrows* points to the many vacuoles that could be detected in the cytoplasm (*left*, magnification, ×400). The induced cells (*middle*) and non-induced cells (*right*) were stained with Oil Red O, suggesting that the vacuoles were adipo-vacuoles (magnification, ×1,000)

($n = 4$) primary clones and 5×10^5 ($n = 4$) or 5×10^4 ($n = 4$) subclones from MThFOB1.19 cells were implanted subcutaneously (s.c.) into nude mice. After 2 weeks, tumors were observed from all injection sites. Histology of s.c. tumors showed that these tumors contained numerous hyperchromatic nuclei with pleomorphism and abundant necrosis (Fig. 2a, right). These results indicated that the MThFOB1.19 cell line is mainly composed of T-ICs.

The capability to self renew is one of the defining features of T-ICs. Thus, serial sarcosphere formation assays were used to detect the self-renewing properties of MThFOB1.19 cells. Primary sphere cells were dissociated and planted into 6-well plates to form secondary spheres in fresh stem cell culture medium. After 4–5 days, the secondary spheres were formed at a rate of 92.64 ± 10.63 %. Moreover, the secondary sarcospheres could be passaged for many generations in stem cell culture medium. Although OS T-ICs lack specific markers, Nanog, Oct4 and Sox2 are thought to be specifically expressed in sarcospheres [9, 12, 15]. Indeed, our immunofluorescence analysis revealed that all three of these factors could easily be detected in MThFOB1.19 sarcospheres (Fig. 2b).

The capability to differentiate is another important feature of T-ICs [4], and adipogenic induction was used to detect this potential in MThFOB1.19 cells. Notable morphological changes were observed after culturing in adipogenesis-inducing medium. In contrast to non-induced cells, enlarged cell volume, smaller karyoplasmic ratio and many cytoplasmic vacuoles could be detected in the induced cells (Fig. 2c, left). Oil Red O staining confirmed that these vacuoles were lipid droplets (Fig. 2c, middle), while the non-induced cells had no lipid droplets (Fig. 2c, right).

TSSC3 is lowly expressed in MThFOB1.19 sarcospheres

Previously, we found that low expression of TSSC3 was associated with OS transformation and progression (our unpublished data). In order to further compare the expression level of TSSC3 in MThFOB1.19 cells and its tumor sphere cells, TSSC3 was first detected by real-time PCR. The results showed that the expression of TSSC3 in sarcosphere cells was 3.28-fold lower than that in MThFOB1.19 cells (Fig. 3a), and analysis by immunofluorescence also confirmed this finding (Fig. 3b). These results demonstrated that TSSC3 was progressively downregulated in malignant transformation and OS sarcosphere cells. To further determine the function of TSSC3 in T-ICs tumorigenesis, the Gene Switch™ system was used to significantly upregulate TSSC3 in MThFOB1.19 cells, which was confirmed by RT-PCR and Western blot, respectively ($P < 0.01$, Fig. 3c, d).

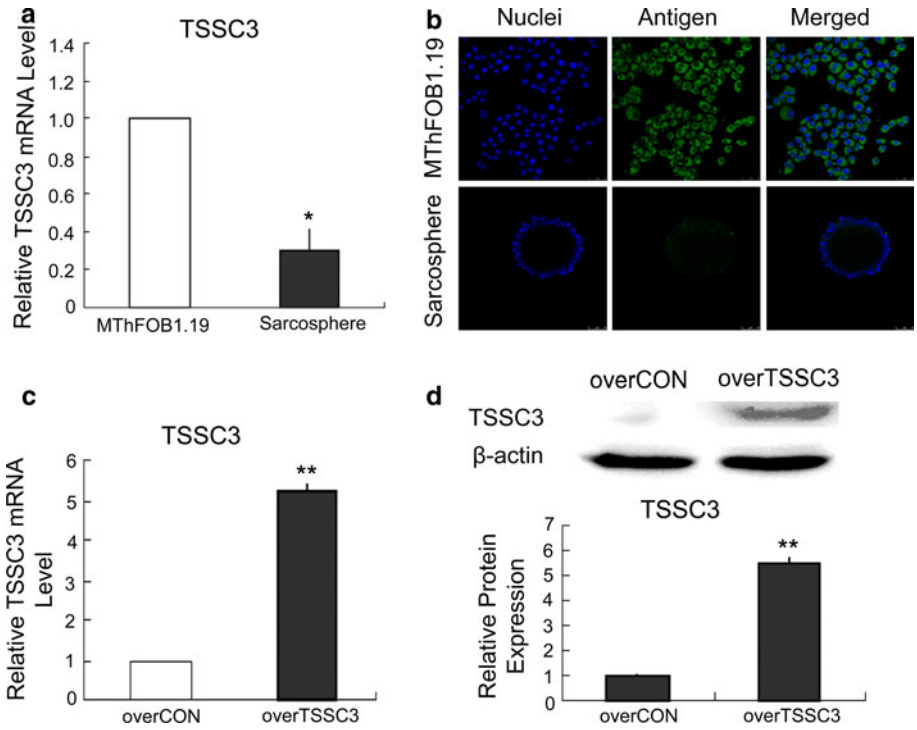

Fig. 3 TSSC3 is lowly expressed in MThFOB1.19 sarcospheres. Real-time PCR (**a**) and immunofluorescence (**b**) showing expression of TSSC3 in both MThFOB1.19 cells and sarcosphere cells, and TSSC3 in MThFOB1.19 was threefold higher than that in tumor sphere cells ($P < 0.01$, *bars*, SD). Real-time PCR (**c**) and Western blot (**d**) demonstrating that TSSC3 was significantly upregulated as much as fivefold when transfected into MThFOB1.19 cells using the GeneSwitch System. $^{**}P < 0.01$ vs. control cells; *bars*, SD

Overexpression of TSSC3 inhibits sarcosphere formation, clone formation in vitro and tumorigenesis in vivo

In order to observe the effect of TSSC3 on sarcosphere formation, TSSC3 overexpressing (overTSSC3) and control (overCON) cells were seeded into 96-well plates containing stem cell medium. After 2 weeks, although sarcospheres were observed in both overTSSC3 cells and overCON cells, overTSSC3 cells had a low sarcosphere formation rate (46.82 ± 8.37 %) relative to the control (66.12 ± 9.36 %), as shown in Fig. 4a ($P < 0.05$). The clone formation assay, which can reflect the tumorigenicity of cells in vitro, was then used to analyze the overTSSC3 cells. OverTSSC3 cells and overCON cells were planted into 96-well plates with 1 cell per well and cultured with serum-containing medium. After 2 weeks, the colony formation rate of overTSSC3 cells was 57.57 ± 2.16 % (Fig. 4b, top), significantly lower than that of control cells (95.32 ± 4.58 %, $P < 0.05$). In addition, the overTSSC3 clones contained fewer cells than the overCON clones (Fig. 4b, bottom). OverTSSC3 and overCON derived clones were randomly selected and expanded. Subsequently, the overTSSC3 (5×10^5) and overCON (5×10^5) clonal cells were implanted s.c. into nude mice ($n = 4$ per group). Only one of four mice implanted with overTSSC3 clonal cells developed a tumor, while overCON clonal cells ($n = 4$) formed more rapidly growing tumors in the all of the mice inoculated (Table 2). Tumors produced by the overCON clonal cells grew fast and reached a diameter of 1.5 cm in 6 weeks after injection, while the tumor produced by overTSSC3 clonal cells grew much more slowly and only reached a diameter of 0.7 cm in 6 weeks (Fig. 4c). In other words, tumors of ~0.7 cm in diameter were achieved for overTSSC3 clonal cells over 6 weeks, compared with a diameter of ~1.5 cm for the controls in the same period, indicating that the mean size of overTSSC3 clonal cell-derived tumors was reduced by 78.56 % at 6 weeks.

Overexpression TSSC3 reduces the expression of stem cell markers Nanog, Oct4 and Sox2

Constitutive expression of Nanog maintains the self-renewal and propagation of cells [20], and together with Oct4 and Sox2 to maintain pluripotency of embryo stem cells [22–24]. To determine whether the expression of TSSC3 can impact the expression of these factors in sarcosphere cells, real-time PCR analyses were carried out. Compared with control sarcosphere cells (overCON-sphere), overTSSC3 sarcosphere (overTSSC3 sphere) cells had lower expressions of Nanog, Sox2 and Oct4 at the transcriptional level (Fig. 4d). Specifically, the expression of Nanog in overTSSC3 sphere cells was downregulated by approximately 80 % ($P < 0.01$), compared with that of overCON sphere cells. Oct4 and Sox2 were downregulated by approximately 20 and 40 % relative to controls, respectively.

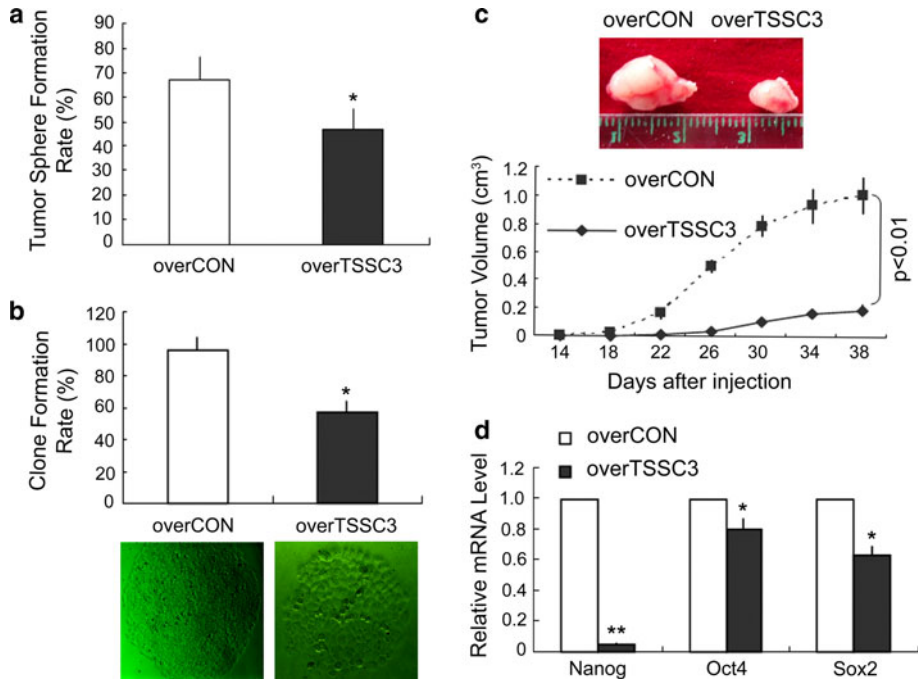

Fig. 4 Overexpression of TSSC3 inhibits sarcosphere formation, colony formation in vitro, reduced tumorigenesis in vivo and downregulated expression of stem cell markers Nanog, Oct4 and Sox2. **a** Sarcosphere formation rate of TSSC3 overexpressing cells (overTSSC3, 46.82 ± 8.37 %) and control cells (overCON, 66.12 ± 9.36 %) indicated that TSSC3 significantly reduced sarcosphere formation ($P < 0.05$; *bars*, SD). **b** The clone formation rate of TSSC3 overexpression cells was 57.57 ± 2.16 %, significantly lower than that of control cells (95.32 ± 4.58 %, $P < 0.05$; *bars*, SD, *top*). In addition, overTSSC3 colonies contained fewer cells than the overCON colonies (*bottom*, magnification, ×100). **c** Tumor volume of TSSC3 overexpression cells was much smaller than control cells. Representative tumors (*top*) and tumor growth curves (*bottom*) are shown from nude mice injected with overCON and overTSSC3 cells ($P < 0.01$; *bars*, SD). **d** Stem cell markers Nanog, Oct4 and Sox2 in overTSSC3 sarcosphere cells were downregulated by approximately 80, 20 and 40 % compared to controls, respectively. *$P < 0.05$ vs. control cells; *bars*, SD

Table 2 In vivo tumor formation from single cell clones in xenografting model

Cell type	Cell numbers per injection	Number of tumors/number of mice injected
OverCON	5×10^5	4/4
OverTSSC3	5×10^5	1/4

Overexpression TSSC3 promotes apoptosis by activating the intrinsic cell apoptotic pathway

TSSC3 was originally identified as a human apoptosis-related imprinted gene. To evaluate the apoptosis-related function of TSSC3 in sarcosphere cells, we performed AnnexinV—APC and PI staining. Relative to the controls, early apoptotic (lower right) and late apoptotic (upper right) cells were both prominently increased from 1.14 and 1.47 % to 7.61 and 6.40 % in overTSSC3-sphere cells, respectively (Fig. 5a). Two signaling pathways are implicated in the apoptotic cascade, the intrinsic (also known as mitochondrial pathway) and extrinsic (also known as death receptor pathway) pathways. To further study the mechanisms involved in TSSC3 induced apoptosis in overTSSC3 sphere cells, common molecules, intrinsic molecules and extrinsic molecules were detected. As shown in Fig. 5b, RT-PCR analysis revealed that upregulation of TSSC3 obviously increased the expression of caspase3, a downstream effector and common molecule of the apoptosis pathway, and increased the expression of Bak, Bim, Cyt *c*, Apaf-1, Noxa, Puma, indicators of intrinsic pathway activation, as well as the Bax: Bcl-2 ratio, which plays an important role in determining the intrinsic pathway. Western blotting analysis also showed increased Cyt *c* and decreased pro-caspase-3 expression (Fig. 5c). The immunofluorescence assay also showed that overTSSC3 sphere cells expressed increased levels of cleaved caspase-3 and decreased levels of pro-caspase-9 (Fig. 5d). As for extrinsic signaling molecules, Fas was slightly upregulated by 1.28 fold, FasL were can't be detected, and Flip was significantly increased by 2.47 fold in overTSSC3 sphere cells compared with the control at the transcriptional level (Fig. 5b, bottom). However the expression of pro-caspase-8, a downstream effector of extrinsic pathway, was not obviously different from control (Fig. 5d).

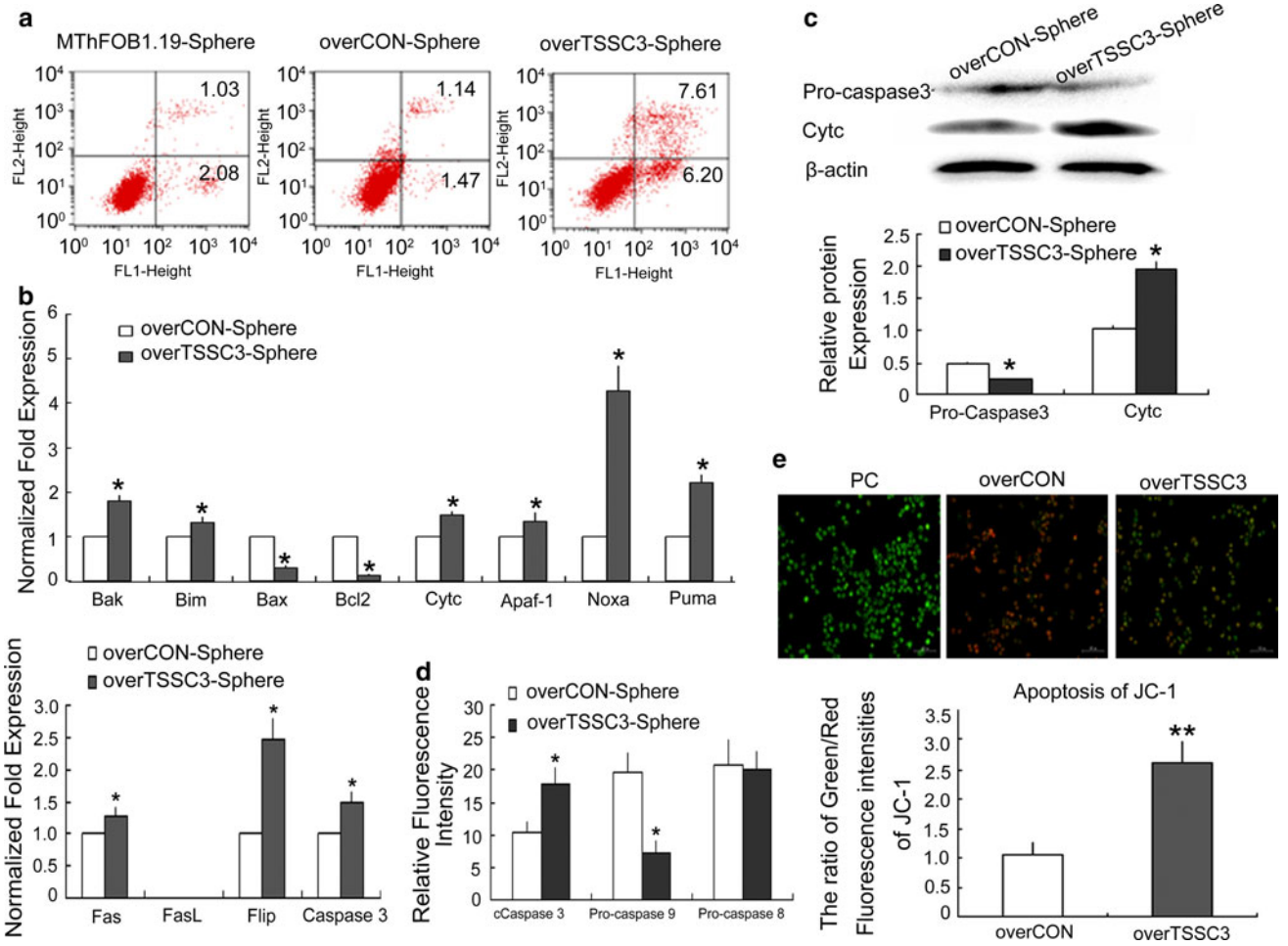

Fig. 5 Overexpression of TSSC3 increases basal apoptosis by activating intrinsic cell apoptotic pathways. **a** Overexpression of TSSC3 (overTSSC3 sphere cells, *right*) increased apoptosis by approximately sixfold compared with controls, MThFOB1.19 sarcosphere cells (*left*) and overCON-sphere cells (*middle*). Percentages of early apoptotic cells (*lower right*) and late apoptotic or necrotic cells (*upper right*) were calculated. Data shown are representative of three independent experiments. **b** The expression of Bak, Bim, Bax, Bcl2, Cytc, Apaf-1, Noxa, Puma, Fas/FasL, Flip and Caspase3 in transcriptional level when TSSC3 was upregulated. $*P < 0.05$ vs. control cells; *bars*, SD. **c** Western blotting revealed that Cyt *c* was upregulated and pro-caspase-3 was downregulated. **d** Immunofluorescence indicated that overTSSC3 sphere cells expressed increased levels of cleaved caspase-3, and decreased level of pro-caspase-9, while no significant difference of Pro-caspase-8. $*P < 0.05$ vs. control cells; *bars*, SD. **e** Mitochondrial transmembrane potential was analyzed in overTSSC3 and overCON sphere cells by using a Mitochondrial Membrane Potential Assay Kit with JC-1. The graph represents the ratio of *green/red fluorescence* intensities of JC-1 from overCON and overTSSC3 sphere cells. Values shown are means ± SD of three independent experiments. $**P < 0.01$; *bars*, SD

Apoptotic signal transduction via the intrinsic pathway is initiated by mitochondrial damage that triggers a disruption of the mitochondrial $\Delta\Psi$, resulting in membrane permeabilization and the release of apoptogenic factors such as Cyt *c* from the mitochondria [25, 26]. To further confirm that the increased expression level of Cyt *c* was concomitant with its translocation from the mitochondria to cytosol, we used the lipophilic cationic agent JC-1 to evaluate changes in TSSC3 expression in sphere cells. Red fluorescence represents the mitochondrial aggregate form of JC-1 with high $\Delta\Psi$ in normal cells. Green fluorescence represents the monomeric form of JC-1 with low $\Delta\Psi$ in apoptotic cells. The ratio of green/red fluorescence intensities of JC-1 was scored as the apoptotic level by the release of Cyt *c*. As shown in Fig. 5e, the overTSSC3 sphere cells had a significantly increased ratio of green/red fluorescence intensities of JC-1 from 1.06 ± 0.21 to 2.61 ± 0.36 ($P < 0.01$). All these results demonstrated that TSSC3 increases basal apoptosis mainly by activation of the intrinsic pathway.

Discussion

The TSC or T-IC theory hypothesizes that tumors of various origins are driven and sustained by a small proportion

of TSCs or T-ICs [2–5]. Previous studies suggest that in some cases T-ICs are derived from somatic stem cells, which are often the target of genetic events for malignant transformation [5, 6, 27]. In other cases, T-ICs are derived from restricted progenitors or even differentiated cells [28, 29]. It is believed that T-ICs arising from transformation of somatic stem cells yield more aggressive cancers than those derived from more committed progenitor cells [27]. As for OS, T-ICs may arise from the committed osteoprogenitor cells, pre-osteoblast cells and early osteoblast cells due to disruption of osteogenic differentiation [7]. In this study we successfully enriched T-ICs by stem cell medium culture of the MThFOB1.19 cell lines, suggesting that OS T-ICs can originate from more differentiated osteoblast cells, consistent with the theory that cancer may be the result of reprogramming of a more differentiated cell type [6, 30]. The tumor sphere formation rate of MThFOB1.19 was found to be much higher than those of SaOS2 and MG63, revealing that the T-ICs are not a small subset in MThFOB1.19 cells. Although studies on diverse cancers revealed that only a few cells were tumorigenic, this may not be a universal phenomenon for all types of cancers [31]. Furthermore, the frequency of T-ICs appears to be highly variable among tumors of the same type [27]. Mathematical analyses have also indicated that T-ICs in advanced tumors may not occur as a small fraction [32]. Quintana et al. [33] found that in limiting dilution assays, approximately 25 % of unselected melanoma cells from different patients formed tumors when injected into highly immunocompromised mice. Zheng et al. [21] also reported that most C6 cells are cancer stem cells by clonal and population analyses rather than isolation based on specific markers. They also demonstrated that serum-free medium is not necessary for the generation of a cancer stem cell clone. Therefore, clonal and population analyses were used to investigate the proportion of T-ICs present in MThFOB1.19 cells. Our data indicated that nearly every MThFOB1.19 cell could generate primary clonal and subclonal populations. Additionally, all clones and subclones could generate tumors when xenotransplanted into nude mice. Like the tumor sphere cells, the MThFOB1.19 cells expressed stem cell markers at both transcriptional and translational levels and could also be induced to differentiate. As T-ICs are cells capable of giving rise to a tumor [34], we thus concluded from the results above that the MThFOB1.19 cell line is mainly composed of T-ICs.

MThFOB1.19 cells were originally obtained by treating human osteoblast hFOB1.19 cells with *N*-methyl-*N*′-nitro-*N*-nitrosoguanidine (MNNG) and 12-O-tetradecanoyl phorbol-13-acetate (TPA) [17]. In this procedure, obvious changes in the expression of imprinted oncogenes and tumor-suppressor genes were observed by oligonucleotide microarrays. Among the imprinted genes identified, TSSC3 (located within the tumor suppressor region of 11p15 [35]), which is implicated in Fas expression and apoptosis, was the first apoptosis-related gene shown to be imprinted [36]. Earlier studies showed that inactivation of TSSC3 can block Fas-mediated apoptosis in breast cancer [37, 38], and its expression is suppressed in several malignant tumors [39, 40]. Here, we found that the expression of TSSC3 was progressively downregulated in malignant transformation [19] and the processes of sarcosphere formation (as shown in "Results"). In order to confirm the function of TSSC3 in T-ICs, TSSC3 overexpression vectors were transfected into MThFOB1.19 cells. The selection of MThFOB1.19 cells for these studies was based on three major pieces of evidence: (a) The ability to form tumors of SaOS2 and MG63 cell lines in xenotransplantation is significantly lower than that of the MThFOB1.19 cell line, consistent with our results in this study (data not shown). (b) MThFOB1.19 cell line was malignantly transformed from differentiated osteoblasts, mainly composed of T-ICs. (c) The expression of TSSC3 was progressively downregulated in the process of malignant transformation of MTF hFOB1.19 and its ability to form spheres. These features of the MThFOB1.19 cell line supported its utilization for our OS tumorigenesis study.

Evidence has emerged that T-ICs are responsible for tumorigenesis [41], and it has been proposed that a tumor is an aberrant organ initiated by a T-IC, which has extensive proliferative potential and the ability to give rise to abnormal tissue [27]. In vivo, T-ICs maintain tumor masses by asymmetrically dividing to produce new T-ICs with the capability to self-renew and generate progenitor cells with the ability to differentiate and proliferate. T-ICs are defined as "a small subset of cancer cells within a cancer that constitute a reservoir of self-sustaining cells with the exclusive ability to self-renew and to cause the heterogeneous lineages of cancer cells that comprise the tumor" [42], and therefore, targeting T-ICs holds enormous therapeutic implications. In this study, overexpression of TSSC3 reduced T-ICs' stemness, such as downregulated the sarcosphere formation, which has been widely used to assess cancer stem cell characteristics, and clone formation abilities, as well as the tumorigenic potential, suggesting overexpression of TSSC3 as a cancer treatment approach. Meanwhile, overexpression TSSC3 also downregulated the expression of stem cell markers Nanog, Oct4 and Sox2 in sarcosphere cells, which have pivotal roles in embryonic stem cells (ESCs) and T-ICs. Nanog, which declined the most among these markers, is essential for early embryonic development and maintaining the stem cell phenotype [20], allowing self renewal. Nanog together with Oct4 and Sox2 can convert human somatic cells into pluripotent stem cells [23, 43]. Decreased Nanog expression correlates with the failure to maintain pluripotent stem cells [44], while enforced Nanog expression can promote de-differentiation

of p53-deficient mouse astrocytes into cancer stem-like cells [28]. Oct4 and Sox2 also play a critical role in the maintenance of pluripotency in ESCs. Loss of expression of Oct4 is associated with differentiation of cells [45]. In tumors, Oct4 maintains the survival of breast cancer stem-like cells, while reduction of Oct4 expression induces T-ICs apoptosis via the Oct4/Tcl1/Akt1 pathway and inhibits tumor growth [46]. In bladder cancer, it was reported that tumors with high expression of Oct4 are associated with further progression, greater metastasis and shorter survival compared with low Oct4 expressing tumors [47]. Overexpression of Sox2 promotes tumorigenesis and increases anti-apoptotic properties, while downregulation of Sox2 decreases tumorigenesis and increases apoptotic sensitivity in human prostate cancer cells [48]. Here, overexpression of TSSC3 decreased the sarcosphere and clone formation abilities and the expression of stem cells markers Nanog, Oct4 and Sox2, indicating that overexpression TSSC3 is an efficient way to downregulate the stem-like features of T-ICs.

T-ICs are more resistant to apoptosis than differentiated cancer cells [49, 50], which can be attributed to diverse molecular changes, such as activation of anti-apoptotic factors, inactivation of pro-apoptotic factors and upregulation of survival signals. These anti-apoptotic properties protect T-ICs from apoptosis and eventually lead to recurrence. Overcome apoptosis resistance of T-ICs is a useful tactics in cancer therapies [8]. In this study, we found that overexpression of TSSC3 induced sarcosphere cells of OS apoptosis significantly, implying TSSC3 may be a promising approach to overcome apoptosis resistance of T-ICs in OS. Lee [18] reported that co-expression of TSSC3 and Fas in multiple human tissues, implicating TSSC3 in Fas-mediated apoptosis. While we previously found that TSSC3 could enhance the mitochondrial-mediated apoptotic pathway in SaOS2 cell line [19]. Here we also found that TSSC3 activated molecules of BH3-only proteins, such as Bak, Bim, Noxa, Puma, downregulated of survival signals Bcl-2 of the mitochondrial pathway, and increased Bax: Bcl-2 ratio, subsequently disrupted the mitochondrial $\Delta\Psi$, released Cyt *c* which combined with Apaf-1 and formed apoptosome, finally activated Caspase3 in MThFOB1.19 sphere cells, suggesting that TSSC3 could enhance the intrinsic apoptotic pathway in OS T-ICs. Interestingly, we found although Fas and Flip were both upregulated, it was reported that malignant cells fail to activate the death receptor pathway is due to the overexpression of Flip despite continued upregulation Fas and FasL [51, 52], moreover, in our study TSSC3 induced Flip overexpression more obviously than Fas. Additionally, recent studies revealed that apart from a killer, Fas has a growth-promoting role during tumorigenesis by a totally different mechanism [53, 54]. However, in this study there was no FasL expression detected in transcriptional level of MThFOB1.19 sarcosphere cells, suggesting that the Fas/FasL signaling pathway has no function in TSSC3 induced apoptosis in OS T-ICs, correspondence with the finding that the downstream molecule pro-caspase-8 which initiates the extrinsic pathways showed no significant changes compared with the control. All the results suggested the extrinsic pathway may not involve in TSSC3-mediated apoptosis. Therefore, we concluded that TSSC3-induced apoptosis mainly occurs by activating intrinsic cell apoptotic pathways, at least in MThFOB1.19 sphere cells.

In conclusion, our study provides preliminary evidence for the first time that OS T-ICs can originate from more differentiated cells, while overexpression of TSSC3 can efficiently decrease tumorigenesis by downregulating stem cell-like features and promoting cell apoptosis though intrinsic apoptosis pathways. Additional studies to clarify the exact mechanism of TSSC3 downregulation of stem cell-like features will be highly valuable for finding new therapeutic strategies to treat OS.

Acknowledgments This study was supported by the National Basic Research Program of China (973 Program, No. 2010CB529402) and the National Natural Science Foundation of China (No. 30971139 and No. 81172554). We thank Professor Cheng Qian (Institute for Pathology and Cancer Research, Southwest Hospital, Chongqing, China) for kindly providing the GeneSwitch™ system (Invitrogen, USA).

Conflict of interest None declared.

References

1. Bonnet D, Dick JE (1997) Human acute myeloid leukemia is organized as a hierarchy that originates from a primitive hematopoietic cell. Nat Med 3(7):730–737
2. Al-Hajj M, Wicha MS, Benito-Hernandez A, Morrison SJ, Clarke MF (2003) Prospective identification of tumorigenic breast cancer cells. Proc Natl Acad Sci U S A 100(7):3983–3988. doi:10.1073/pnas.0530291100
3. Pardal R, Clarke MF, Morrison SJ (2003) Applying the principles of stem-cell biology to cancer. Nat Rev Cancer 3(12):895–902. doi:10.1038/nrc1232
4. Singh SK, Clarke ID, Terasaki M, Bonn VE, Hawkins C, Squire J, Dirks PB (2003) Identification of a cancer stem cell in human brain tumors. Cancer Res 63(18):5821–5828
5. Reya T, Morrison SJ, Clarke MF, Weissman IL (2001) Stem cells, cancer, and cancer stem cells. Nature 414(6859):105–111. doi:10.1038/35102167
6. Davies EJ, Marsh V, Clarke AR (2011) Origin and maintenance of the intestinal cancer stem cell. Mol Carcinog 50(4):254–263. doi:10.1002/mc.20631
7. Tang N, Song WX, Luo J, Haydon RC, He TC (2008) Osteosarcoma development and stem cell differentiation. Clin Orthop Relat Res 466(9):2114–2130. doi:10.1007/s11999-008-0335-z
8. Signore M, Ricci-Vitiani L, De Maria R (2011) Targeting apoptosis pathways in cancer stem cells. Cancer Lett. doi:10.1016/j.canlet.2011.01.013

9. Gibbs CP, Kukekov VG, Reith JD, Tchigrinova O, Suslov ON, Scott EW, Ghivizzani SC, Ignatova TN, Steindler DA (2005) Stem-like cells in bone sarcomas: implications for tumorigenesis. Neoplasia 7(11):967–976
10. Tirino V, Desiderio V, d'Aquino R, De Francesco F, Pirozzi G, Graziano A, Galderisi U, Cavaliere C, De Rosa A, Papaccio G, Giordano A (2008) Detection and characterization of CD133+ cancer stem cells in human solid tumours. PLoS ONE 3(10): e3469. doi:10.1371/journal.pone.0003469
11. Veselska R, Hermanova M, Loja T, Chlapek P, Zambo I, Vesely K, Zitterbart K, Sterba J (2008) Nestin expression in osteosarcomas and derivation of nestin/CD133 positive osteosarcoma cell lines. BMC Cancer 8:300. doi:10.1186/1471-2407-8-300
12. Wilson H, Huelsmeyer M, Chun R, Young KM, Friedrichs K, Argyle DJ (2008) Isolation and characterisation of cancer stem cells from canine osteosarcoma. Vet J 175(1):69–75. doi:10.1016/j.tvjl.2007.07.025
13. Di Fiore R, Santulli A, Ferrante RD, Giuliano M, De Blasio A, Messina C, Pirozzi G, Tirino V, Tesoriere G, Vento R (2009) Identification and expansion of human osteosarcoma-cancer-stem cells by long-term 3-aminobenzamide treatment. J Cell Physiol 219(2):301–313. doi:10.1002/jcp21667
14. Cheng L, Sung MT, Cossu-Rocca P, Jones TD, MacLennan GT, De Jong J, Lopez-Beltran A, Montironi R, Looijenga LH (2007) OCT4: biological functions and clinical applications as a marker of germ cell neoplasia. J Pathol 211(1):1–9. doi:10.1002/path.2105
15. Tang QL, Zhao ZQ, Li JC, Liang Y, Yin JQ, Zou CY, Xie XB, Zeng YX, Shen JN, Kang T, Wang J (2011) Salinomycin inhibits osteosarcoma by targeting its tumor stem cells. Cancer Lett 311(1):113–121. doi: 10.1016/j.canlet.2011.07.016
16. Pece S, Tosoni D, Confalonieri S, Mazzarol G, Vecchi M, Ronzoni S, Bernard L, Viale G, Pelicci PG, Di Fiore PP (2010) Biological and molecular heterogeneity of breast cancers correlates with their cancer stem cell content. Cell 140(1):62–73. doi: 10.1016/j.cell.2009.12.007
17. Li Y, Meng G, Guo QN (2008) Changes in genomic imprinting and gene expression associated with transformation in a model of human osteosarcoma. Exp Mol Pathol 84(3):234–239. doi: 10.1016/j.yexmp.200803013
18. Lee MP, Feinberg AP (1998) Genomic imprinting of a human apoptosis gene homologue, TSSC3. Cancer Res 58(5):1052–1056
19. Dai H, Huang Y, Li Y, Meng G, Wang Y, Guo QN (2012) TSSC3 overexpression associates with growth inhibition, apoptosis induction and enhances chemotherapeutic effects in human osteosarcoma. Carcinogenesis 33(1):30–40. doi:10.1093/carcin/bgr232
20. Silva J, Nichols J, Theunissen TW, Guo G, van Oosten AL, Barrandon O, Wray J, Yamanaka S, Chambers I, Smith A (2009) Nanog is the gateway to the pluripotent ground state. Cell 138(4):722–737. doi:10.1016/j.cell.2009.07.039
21. Zheng X, Shen G, Yang X, Liu W (2007) Most C6 cells are cancer stem cells: evidence from clonal and population analyses. Cancer Res 67(8):3691–3697. doi:10.1158/0008-5472.can-06-3912
22. Meissner A, Wernig M, Jaenisch R (2007) Direct reprogramming of genetically unmodified fibroblasts into pluripotent stem cells. Nat Biotechnol 25(10):1177–1181. doi:10.1038/nbt1335
23. Okita K, Ichisaka T, Yamanaka S (2007) Generation of germline-competent induced pluripotent stem cells. Nature 448(7151): 313–317. doi:10.1038/nature05934
24. Pei D (2009) Regulation of pluripotency and reprogramming by transcription factors. J Biol Chem 284(6):3365–3369. doi:10.1074/jbc.R800063200
25. Su X, Zheng X, Ni J (2009) Lanthanum citrate induces anoikis of Hela cells. Cancer Lett 285(2):200–209. doi:10.1016/j.canlet.2009.05.018
26. Zhu XJ, Shi Y, Peng J, Guo CS, Shan NN, Qin P, Ji XB, Hou M (2009) The effects of BAFF and BAFF-R-Fc fusion protein in immune thrombocytopenia. Blood 114(26):5362–5367. doi:10.1182/blood-2009-05-217513
27. Visvader JE, Lindeman GJ (2008) Cancer stem cells in solid tumours: accumulating evidence and unresolved questions. Nat Rev Cancer 8(10):755–768. doi:10.1038/nrc2499
28. Moon JH, Kwon S, Jun EK, Kim A, Whang KY, Kim H, Oh S, Yoon BS, You S (2011) Nanog-induced dedifferentiation of p53-deficient mouse astrocytes into brain cancer stem-like cells. Biochem Biophys Res Commun 412(1):175–181. doi:10.1016/j.bbrc.2011.07.070
29. Scaffidi P, Misteli T (2011) In vitro generation of human cells with cancer stem cell properties. Nat Cell Biol 13(9):1051–1061. doi:10.1038/ncb2308
30. Trosko JE (2009) Review paper: cancer stem cells and cancer non-stem cells: from adult stem cells or from reprogramming of differentiated somatic cells. Vet Pathol 46(2):176–193. doi:10.1354/vp.462176
31. Li F (2009) Every single cell clones from cancer cell lines growing tumors in vivo may not invalidate the cancer stem cell concept. Mol Cells 27(4):491–492. doi:10.1007/s10059-009-0056-5
32. Kern SE, Shibata D (2007) The fuzzy math of solid tumor stem cells: a perspective. Cancer Res 67(19):8985–8988. doi:10.1158/0008-5472.can-07-1971
33. Quintana E, Shackleton M, Sabel MS, Fullen DR, Johnson TM, Morrison SJ (2008) Efficient tumour formation by single human melanoma cells. Nature 456(7222):593–598. doi:10.1038/nature07567
34. Oliver TG, Wechsler-Reya RJ (2004) Getting at the root and stem of brain tumors. Neuron 42(6):885–888. doi:10.1016/j.neuron.2004.06.011
35. Hu RJ, Lee MP, Connors TD, Johnson LA, Burn TC, Su K, Landes GM, Feinberg AP (1997) A 2.5-Mb transcript map of a tumor-suppressing subchromosomal transferable fragment from 11p15.5, and isolation and sequence analysis of three novel genes. Genomics 46(1):9–17. doi:10.1006/geno.1997.4981
36. Qian N, Frank D, O'Keefe D, Dao D, Zhao L, Yuan L, Wang Q, Keating M, Walsh C, Tycko B (1997) The IPL gene on chromosome 11p15.5 is imprinted in humans and mice and is similar to TDAG51, implicated in Fas expression and apoptosis. Hum Mol Genet 6(12):2021–2029
37. Keane MM, Ettenberg SA, Lowrey GA, Russell EK, Lipkowitz S (1996) Fas expression and function in normal and malignant breast cell lines. Cancer Res 56(20):4791–4798
38. Nagai MA, Fregnani JH, Netto MM, Brentani MM, Soares FA (2007) Down-regulation of PHLDA1 gene expression is associated with breast cancer progression. Breast Cancer Res Treat 106(1):49–56. doi:10.1007/s10549-006-9475-6
39. Muller S, van den Boom D, Zirkel D, Koster H, Berthold F, Schwab M, Westphal M, Zumkeller W (2000) Retention of imprinting of the human apoptosis-related gene TSSC3 in human brain tumors. Hum Mol Genet 9(5):757–763
40. Schwienbacher C, Angioni A, Scelfo R, Veronese A, Calin GA, Massazza G, Hatada I, Barbanti-Brodano G, Negrini M (2000) Abnormal RNA expression of 11p15 imprinted genes and kidney developmental genes in Wilms' tumor. Cancer Res 60(6): 1521–1525
41. Frank NY, Schatton T, Frank MH (2010) The therapeutic promise of the cancer stem cell concept. J Clin Invest 120(1):41–50. doi: 10.1172/jci41004
42. Clarke MF, Dick JE, Dirks PB, Eaves CJ, Jamieson CH, Jones DL, Visvader J, Weissman IL, Wahl GM (2006) Cancer stem cells—perspectives on current status and future directions:

AACR workshop on cancer stem cells. Cancer Res 66(19): 9339–9344. doi:10.1158/0008-5472.can-06-3126
43. Peng S, Maihle NJ, Huang Y (2010) Pluripotency factors Lin28 and Oct4 identify a sub-population of stem cell-like cells in ovarian cancer. Oncogene 29(14):2153–2159. doi:10.1038/onc.2009.500
44. Mitsui K, Tokuzawa Y, Itoh H, Segawa K, Murakami M, Takahashi K, Maruyama M, Maeda M, Yamanaka S (2003) The homeoprotein Nanog is required for maintenance of pluripotency in mouse epiblast and ES cells. Cell 113(5):631–642
45. Sell S (2004) Stem cell origin of cancer and differentiation therapy. Crit Rev Oncol Hematol 51(1):1–28. doi:10.1016/j.critrevonc.2004.04.007
46. Hu T, Liu S, Breiter DR, Wang F, Tang Y, Sun S (2008) Octamer 4 small interfering RNA results in cancer stem cell-like cell apoptosis. Cancer Res 68(16):6533–6540. doi:10.1158/0008-5472.can-07-6642
47. Chang CC, Shieh GS, Wu P, Lin CC, Shiau AL, Wu CL (2008) Oct-3/4 expression reflects tumor progression and regulates motility of bladder cancer cells. Cancer Res 68(15):6281–6291. doi:10.1158/0008-5472.can-08-0094
48. Jia X, Li X, Xu Y, Zhang S, Mou W, Liu Y, Lv D, Liu CH, Tan X, Xiang R, Li N (2011) SOX2 promotes tumorigenesis and increases the anti-apoptotic property of human prostate cancer cell. J Mol Cell Biol 3(4):230–238. doi:10.1093/jmcb/mjr002
49. Mimeault M, Batra SK (2006) Concise review: recent advances on the significance of stem cells in tissue regeneration and cancer therapies. Stem Cells 24(11):2319–2345. doi:10.1634/stemcells.2006-0066
50. Mimeault M, Hauke R, Mehta PP, Batra SK (2007) Recent advances in cancer stem/progenitor cell research: therapeutic implications for overcoming resistance to the most aggressive cancers. J Cell Mol Med 11(5):981–1011. doi:10.1111/j.1582-4934.2007.00088.x
51. Simpson CD, Anyiwe K, Schimmer AD (2008) Anoikis resistance and tumor metastasis. Cancer Lett 272(2):177–185. doi:10.1016/j.canlet.2008.05.029
52. Mawji IA, Simpson CD, Hurren R, Gronda M, Williams MA, Filmus J, Jonkman J, Da Costa RS, Wilson BC, Thomas MP, Reed JC, Glinsky GV, Schimmer AD (2007) Critical role for Fas-associated death domain-like interleukin-1-converting enzyme-like inhibitory protein in anoikis resistance and distant tumor formation. J Natl Cancer Inst 99(10):811–822. doi:10.1093/jnci/djk182
53. Green DR (2010) Cancer: a wolf in wolf's clothing. Nature 465(7297):433. doi:10.1038/465433a
54. Chen L, Park SM, Tumanov AV, Hau A, Sawada K, Feig C, Turner JR, Fu YX, Romero IL, Lengyel E, Peter ME (2010) CD95 promotes tumour growth. Nature 465(7297):492–496. doi:10.1038/nature09075